O.O. ILCHENKO,[1] A.M. KUTSYK,[2] Y.V. PILGUN,[2] V.V. OBUKHOVSKY,[2] V.V. NIKONOVA [2]

[1] D.F. Chebotarev State Institute of Gerontology, NAMS of Ukraine
(67, Vyshgorods'ka Str., Kyiv 04114, Ukraine)

[2] Taras Shevchenko National University of Kyiv
(64, Volodymyrs'ka Str., Kyiv 01033, Ukraine; e-mail: a.m.kutsyk@gmail.com, vobukhovsky@yandex.ua)

PACS 78.30.C-, 61.25.Em

FORMATION OF MOLECULAR COMPLEXES IN LIQUID BENZENE-CHLOROFORM MIXTURES EXAMINED BY MID-IR 2D CORRELATION SPECTROSCOPY AND MULTIVARIATE CURVE RESOLUTION

Mid-IR spectroscopy is used for the investigation of the formation of molecular complexes in a liquid benzene-chloroform solution. Spectra are measured in the spectral interval 2950–3100 cm^{-1}, which corresponds to CH stretching vibrations of benzene and chloroform. The 2D correlation analysis of spectral data indicates the presence of molecular complexes in the solution. The analysis of residual spectra also supports this conclusion. Model-free and model-based analyses are applied for the decomposition of spectral data. The concentration and spectral profiles of molecular complexes are determined. The analysis shows that a complex consists of one molecule of benzene and one molecule of chloroform.

K e y w o r d s: Mid-IR spectroscopy, benzene, chloroform, complex formation, multivariate curve resolution, 2D correlation spectroscopy.

1. Introduction

Structural changes in liquid solutions predefine their macroscopic physical properties (e.g., viscosity, diffusion, dielectric permittivity, *etc.*) [1]. Liquid solutions are widely used for a modification of the molecular environment in order to arrange the organic synthesis, reaction kinetics, or protein folding [2]. Thus, they allow one to control properties of the system. Another important aspect of the usage of binary liquid solutions is a change of the photobehavior of different solutes (e.g., absorption and fluorescence of some dyes) [3].

For our investigation, we chose a benzene-chloroform liquid solution due to its relative simplicity and availability of alternative experimental investigations. The formation of molecular complexes in liquid benzene-chloroform solution has been investigated widely [4–13], but there is some uncertainty in the description of their structure and stoichiometric composition. A complex is formed due to the hydrogen bond,

and it is suggested to be equimolecular by numerous NMR studies [5–10]. In a benzene-chloroform solution, the chloroform proton resonance is shifted very much to the higher field. Thus, it is interpreted as the formation of a weak hydrogen bond by chloroform with a benzene molecule. The molecule of benzene operates as a π-electron donor. Accordingly, the CH-bond of chloroform is oriented normally to the molecular plane of a benzene molecule. Nevertheless, the molecular dynamics study indicates that such geometry of a complex is not preferred [11, 12]. In addition, the existence of a 1:1 complex is supported by experiments, where the dielectric relaxation in a dilute solution of chloroform with benzene was investigated [13].

The concentration dependence of the excess enthalpy has minimum at 50% mol. of benzene and is an indirect evidence of the equimolecular complex formation [14, 15]. Thermal and volumetric properties of a benzene-chloroform solution were described quantitatively within a model of ideal associated solution, which took the complex formation into account [16].

The investigation of the thermal diffusion indicates that the complex is formed by two molecules of chloroform and one of benzene [17]. Rayleigh scattering studies revealed the more complex structure in a solution including self-associates of benzene and chloroform [4].

The aim of this paper is the investigation of the complex formation in a liquid benzene-chloroform solution by mid-infrared absorption spectroscopy. This spectral range was selected due to its high sensitivity to structural changes occurring in the investigated system [18]. Spectral data were analyzed by means of excess spectroscopy [19, 20], generalized 2D correlation spectroscopy [21], and multivariate curve resolution [22].

2. Theoretical Part

2.1. Analysis of residual spectra (excess spectroscopy)

The analysis of residual spectra is a simple, but, at the same time, useful tool for the investigation of the intermolecular interaction in binary solutions [19, 20, 23, 24]. The main idea is the consideration of deviations from Beer's law. When the excess intermolecular interactions are absent, the spectra of a binary mixture could be represented as a linear combination of the spectra of pure components:

$$S_{ideal} = c_1 S_1 + c_2 S_2. \tag{1}$$

Here, $S_{1,2}$ are the spectra, and $c_{1,2}$ are the concentrations of pure components.

The presence of interactions between mixture components causes deviations from Beer's law, but the observed spectra S_{obs} are not equal to S_{ideal}. Hence, the excess (or residual) spectra S^E can be defined as

$$S^E = S_{obs} - S_{ideal}. \tag{2}$$

The residual spectra S^E represent a non-ideality caused by intermolecular interactions.

2.2. Multivariate curve resolution (MCR)

MCR methods are based on a bilinear model like the one given in [22]:

$$\mathbf{A} = \mathbf{C}\mathbf{S}^T + \mathbf{E}. \tag{3}$$

The goal of MCR is the bilinear decomposition of the data matrix $\mathbf{A}$ (spectra measured during the experiment) into the "true" pure response profiles associated with a variation of each contribution in the row and column directions represented by matrices $\mathbf{C}$ (concentration profiles) and $\mathbf{S}^T$ (spectral profiles), respectively, which are responsible for the observed data variance; $\mathbf{E}$ is the matrix of residuals not explained by the model, and, ideally, it should be close to the experimental error. Among MCR methods, the alternating least squares one (MCR-ALS) [25, 26] turned out to be especially useful and simple to use.

Unfortunately, MCR-ALS solutions are not unique. There are two types of ambiguities related to the rotation and the intensity [22, 26]. The most important is the rotational ambiguity. It always appears, if there are two or more highly overlapped spectra. Hence, the estimated spectra of these components will be arbitrary linear combinations of the true components. The MCR-BANDS method was proposed to decrease the rotational ambiguity [27]. It is based on a nonlinear constrained optimization of an objective function defined by the ratio of the signal contribution of particle species to the whole measured signal.

Another fundamentally different way of extracting the information from spectral data is the model-based analysis [28, 29]. The model-based (or hard-modeling) approaches are based on mathematical relations, which describe the measured data quantitatively. For equilibrium studies, the analysis is based on the law of mass action [29]. Thus, the concentration matrix $\mathbf{C}$ depends on the set of equilibrium constants $\mathbf{C} = \mathbf{C}(\mathbf{K})$, $\mathbf{K} = (K_1, K_2, ..., K_m)$. The set of optimal parameters is found by solving the following problem:

$$\tilde{\mathbf{K}} = \underset{\mathbf{K}}{\operatorname{argmin}} \|\mathbf{D} - \mathbf{C}(\mathbf{K})\mathbf{C}^+(\mathbf{K})\mathbf{D}\|. \tag{4}$$

The most difficult aspect of the hard-modeling is the determination of a correct model. Thus, the model-free methods such as MCR-ALS can be indispensable in supporting the model choice.

2.3. Generalized two-dimensional correlation spectroscopy

The detailed description of generalized two-dimensional correlation spectroscopy (2D COS) can be found in [21, 30, 31]. The 2D COS analysis is based on the cross-correlation of spectral intensity variations induced by an external perturbation, which is imposed on the investigated system. The main advantages of

2D correlation spectroscopy are the following: enhancement of a spectral resolution by spreading peaks along the second dimension and the establishment of unambiguous assignments through the correlation of bands selectively coupled by various interaction mechanisms.

The 2D COS analysis is carried out on the so-called dynamic spectrum $\tilde{A}$, which is a result of the subtraction of the reference spectrum from the raw data:

$$\tilde{A}(\nu, t) = \begin{cases} A(\nu, t) - \bar{A}(\nu), & \text{if } T_{\min} \leq t \leq T_{\max}, \\ 0, & \text{otherwise.} \end{cases} \quad (5)$$

Any perturbation such as time, temperature, concentration, pressure, *etc.* may be used as the external variable t. The average spectrum $\bar{A}$ is usually chosen as a reference spectrum. In this case, the synchronous 2D correlation spectrum $\Phi(\nu_1, \nu_2)$ has the same sense as the covariance matrix $\text{cov}(\tilde{A})$:

$$\Phi(\nu_1, \nu_2) = \frac{1}{m-1} \sum_{j=1}^{m} \tilde{A}(\nu_1, t_j) \tilde{A}(\nu_2, t_j) \equiv \text{cov}(\tilde{A}), \quad (6)$$

where m is equal to the number of measured samples, and t_j is a perturbation variable.

The asynchronous 2D spectrum $\Psi(\nu_1, \nu_2)$, which represents out-of-phase variations of the spectral intensities under external perturbations, is calculated by multiplying the data matrix $\tilde{A}$ and the orthogonal counterpart of $\tilde{A}$ obtained by the Hilbert transformation [21, 31]:

$$\Psi(\nu_1, \nu_2) = \frac{1}{m-1} \sum_{j=1}^{m} \tilde{A}(\nu_1, t_j) \sum_{i=1}^{m} N_{ij} \tilde{A}(\nu_2, t_i). \quad (7)$$

Here, N is the Hilbert–Noda transformation matrix

$$N_{ij} = \begin{cases} 0, & \text{if } i = j, \\ \dfrac{1}{\pi(j-i)} & \text{if } i \neq j. \end{cases} \quad (8)$$

The synchronous and asynchronous spectra can be obtained simply from Eqs. (6) and (7). In spite of the convenient time-series correlation analysis, the generalized 2D cross-spectra are calculated without the Fourier transformation of dynamic spectra [21, 30]. This feature implies the usage of different forms and different kinds of applied external perturbations.

The order of appearance of induced spectral variations as the response to a perturbation is governed by Noda's rules [21]. According to these rules, if the signs of $\Phi(\nu_1, \nu_2)$ and $\Psi(\nu_1, \nu_2)$ are the same, the overall spectral intensity variation observed at ν_1 predominantly occurs prior to that at ν_2. If the signs are different, the order is reversed. If $\Phi(\nu_1, \nu_2) = 0$, the sequential order of intensity variations cannot be determined.

Sometimes, it is worthless to use scaling techniques for the enhancement of important, but subtle spectral features, which obscured by the dominant spectral variations [32]. One of these techniques is the Pareto scaling. It is characterized by dividing the dataset by the square root of its standard deviation. Thus, the Pareto-scaled 2D correlation spectra are defined as

$$\Phi(\nu_1, \nu_2)^{\text{Pareto}} = \Phi(\nu_1, \nu_2) / \sqrt{\sigma(\nu_1)\,\sigma(\nu_2)},$$
$$\Psi(\nu_1, \nu_2)^{\text{Pareto}} = \Psi(\nu_1, \nu_2) / \sqrt{\sigma(\nu_1)\,\sigma(\nu_2)}, \quad (9)$$

where the standard deviation is calculated as

$$\sigma(\nu_i) = \sqrt{\Phi(\nu_i, \nu_i)}. \quad (10)$$

The 2D correlation analysis is useful for the detection of non-linear spectral variations. If the spectral changes are linear and described by Eq. (1), the asynchronous spectrum is zero:

$$\Psi(\nu_1, \nu_2) = 0. \quad (11)$$

3. Experiments

3.1. Samples and instrumentation

The Fourier-transformed infrared spectra (FTIR) were measured, by using a Thermo Scientific Nicolet iS50 FTIR spectrometer with a maximum spectral resolution of 0.125 cm^{-1}. The heating of the sample almost did not occur during the measurements (due to a small value of absorption coefficient). The temperature of liquid samples was 25 ± 0.2 °C. Benzene and chloroform with purity 99.9% were used in this research. The concentration of components was changed from 0% to 100% (in volume %) with a step of 10%. Measurements were carried out in a CaF$_2$ transition cell with an optical pathlength of 15μ. 32 scans were collected for an individual spectrum with a spectral resolution of 4 cm^{-1}. Thereafter, the average spectra were calculated for every concentration and used for the further analysis.

3.2. Computational details

The MCR analysis was carried out, by using MATLAB GUI developed by Tauler's group [33]. The 2D

correlation analysis was performed by the CTH2CSA program in MATLAB environment [1].

4. Results and Discussion

4.1. IR spectra and residual spectra analysis

The FTIR spectra of a chloroform-benzene solution in the spectral range of CH stretching vibrations (2950–3150 cm^{-1}) were chosen for the analysis (Fig. 1). This range was chosen due to a high sensitivity of stretching modes to the hydrogen bonding [18].

The method of analysis of the residual (excess) spectra was applied for the visualization of complex-formation effects (Fig. 2). As we can see from Fig. 2, the concentration distibution of the residual intensity is not random. Hence, it is a clear evidence that the measured spectra cannot be repsented by Eq. (1). The intermolecular interactions (hydrogen bonding) cause the frequency shifts of corresponding vibrations. As a cosequence, this leads to the appearence of the regions with positive residual intensity in excess spectra. In the case of a benzene-chloroform solution, such regions in Fig. 2 correspond to CH stretching vibrations of both chloroform and benzene in bonded state, i.e. as a part of the molecular complex.

4.2. Generalized 2D correlation analysis

The generalized 2D correlation analysis was applied to the measured FTIR spectra. The solution concentration changes were considered as an external perturbation.

The Pareto scaled synchronous and asynchronous spectra are shown in Fig. 3. The presence of intermolecular interactions between mixture components causes the non-linear behavior of spectral variations. Hence, the asynchronous spectrum is not zero. The analysis of both asynchronous and synchronous spectra provides the information about the order of the spectral variations induced by solution concentration changes. The analysis of the order of spectral variations due to Noda's rules is provided in Table 1. The notation $\nu_1 \rightarrow \nu_2$ means that the spectral variation at ν_1 occurs predominantly at lower concentrationa of benzene in the solution than the variation at ν_2.

Analyzing the asynchronous spectra, we can see asynchronously correlated peaks at the range of

---

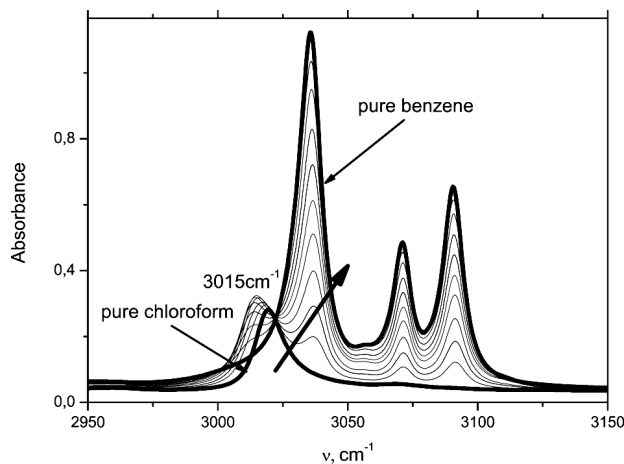[1] MATLAB scripts were kindly provided by Dr. S. Lavoryk.

Fig. 1. FTIR transmission spectra of a benzene-chloroform liquid solution measured at different concentrations. The arrow indicates the spectra transformation due to an increase of the benzene concentration with a step of 10% vol
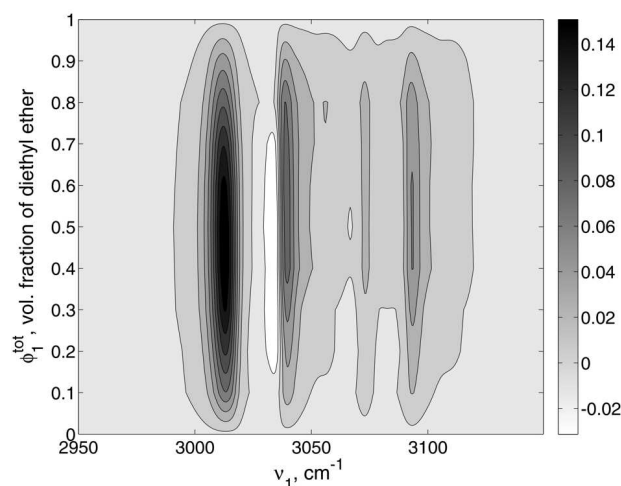

Fig. 2. Contour map of the excess spectra of a benzene-chloroform solution

CH stretching vibrations of benzene: two peaks (3090 cm^{-1}, 3096 cm^{-1}) and two peaks (3034 cm^{-1}, 3041 cm^{-1}) (see corresponding correlation squares in Fig. 3). This is a characteristic spectral pattern, which corresponds to two highly overlapped bands with out-of-phase intensity changes [21]. These two bands can be interpreted as CH stretching vibrations of benzene in two states: unbonded (free) and bonded (in a complex). A similar spectral feature is observed around the CH stretching vibration range of chloroform – (3012 cm^{-1}, 3018 cm^{-1}). It corresponds to
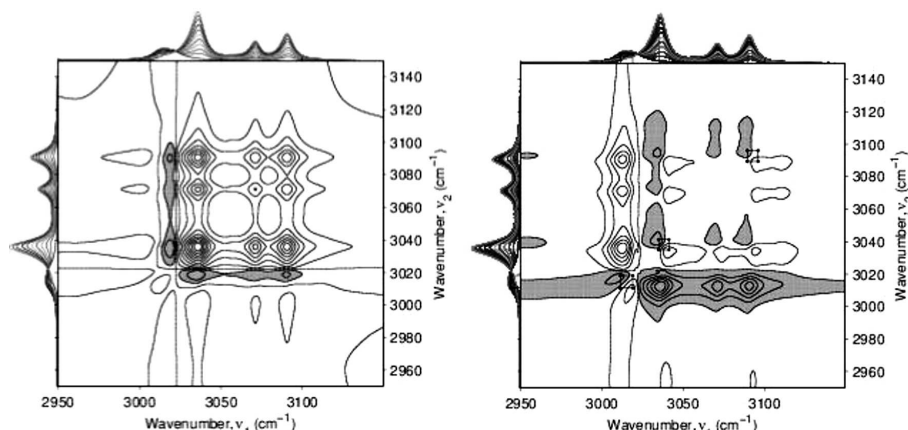
Fig. 3. Pareto-scaled synchronous (left) and asynchronous (right) spectra of benzene-chloroform solutions. (Areas with negative values are shaded)

highly overlapped CH stretching bands of chloroform in the free state and in the complex. Thus, we can conclude that, apart from both unbonded benzene and chloroform, there are chloroform and benzene in the bonded state in the investigated solution.

The application of Noda's rules to these spectral variations gives the following: the spectral variation at 3018 cm^{-1} (which corresponds to pure chloroform) occurs before (at a lower concentration of benzene) changes at 3012 cm^{-1}(which we interpret as a vibration of the molecular complex); the spectral variation at 3090 cm^{-1} (which corresponds to pure benzene) occurs after (at higher concentration of benzene) changes at 3096 cm^{-1} (which we interpret as a vibration of the molecular complex). We have the same interpretation for two correlated peaks (3034 cm^{-1}, 3041 cm^{-1}): the spectral variation at

3034 cm^{-1} (pure benzene) occurs at a higher concentration of benzene in comparison to changes at 3096 cm^{-1} (molecular complex). The order of all spectral variations is given in the Table.

4.3. Multivariate curve resolution

4.3.1. Model-free decomposition

The crucial step in the multivariate curve resolution is the determination of the number of components which are present in the investigated system. As usual, it is determined by the analysis of singular values of the measured spectral matrix **A**. In our case, there are three biggest singular values (see the inner plot in Fig. 4). To be sure, we also determined the so-called informativeness criterion [34]:

$$I_n = \frac{\sum_{i=1}^{n} \sigma_i}{\sum_{i=1}^{n_{\max}} \sigma_i}. \tag{12}$$

It can be seen from Fig. 4 that adding the fourth principal component practically does not change the informativeness. Hence, we can conclude that there are three species in the investigated solution. This conclusion coincides with the previous conclusions obtained by the analysis of residual spectra and the 2D correlation analysis.

We used a three-component model for the spectra decomposition. During the optimization, the prior information about the system, such as the non-negativity in spectra and the concentration, for concentration profiles and the closure condition, was

Order of spectral variations obtained from 2D COS

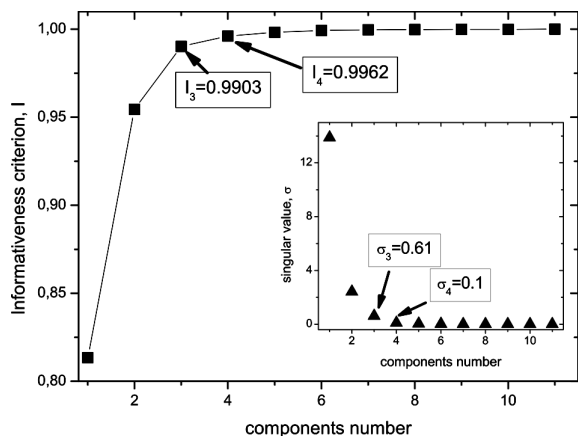| Frequencies (ν_1, ν_2)	sign $\Phi(\nu_1, \nu_2)$	sign $\Psi(\nu_1, \nu_2)$	Spectral variations order
(3012, 3090)	+	+	$\nu_1 \to \nu_2$
(3012, 3072)	+	+	$\nu_1 \to \nu_2$
(3012, 3018)	+	−	$\nu_1 \leftarrow \nu_2$
(3034, 3041)	+	−	$\nu_1 \leftarrow \nu_2$
(3034, 3096)	+	−	$\nu_1 \leftarrow \nu_2$
(3089, 3096)	+	−	$\nu_1 \leftarrow \nu_2$
(3041, 3090)	+	+	$\nu_1 \to \nu_2$
(3041, 3072)	+	+	$\nu_1 \to \nu_2$
(3072, 3096)	+	−	$\nu_1 \leftarrow \nu_2$

Fig. 4. Dependence of the informativeness criterion on the number of components. (Inner plot shows singular values of the spectral data matrix)
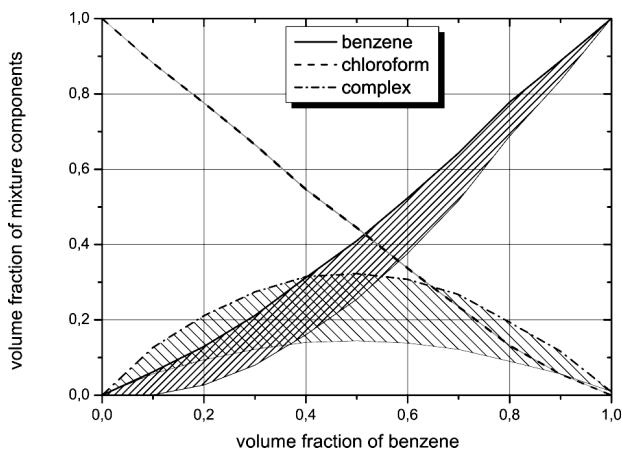

Fig. 5. Concentration profiles of benzene-chloroform mixture components obtained by MCR-BANDS (The shaded area indicates the range of feasible concentration profiles of corresponding mixture components)

Fig. 6. Spectral profiles of benzene-chloroform mixture components obtained by MCR-BANDS (The shaded area indicates the range of feasible spectral profiles of the complex)

Fig. 7. Concentration profiles of benzene-chloroform mixture components obtained by the hard-modeling

applied in the form of constraints. MCR-ALS solutions were used as an initial approximation for the MCR-BANDS optimization. The resulting concentration and spectral profiles are presented in Figs. 5 and 6.

The spectra of the complex and the pure components are highly overlapped and cannot be seen by the usual univariate spectroscopy techniques. Such behavior corresponds to the conclusions obtained from the 2D correlation analysis carried out above. The CH stretching vibration of chloroform in the complex is red-shifted in comparison to such vibration in free chloroform. It can be explained by the lengthening of
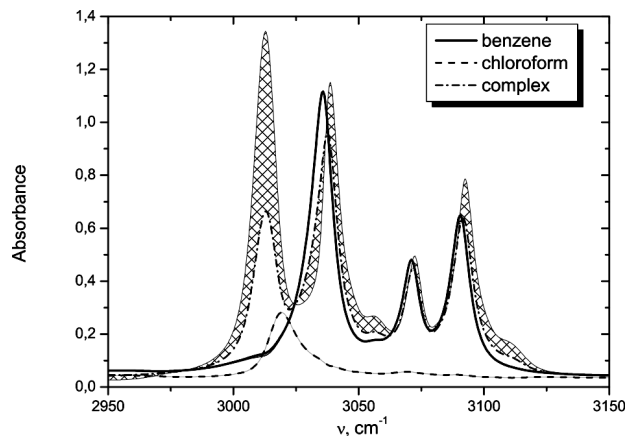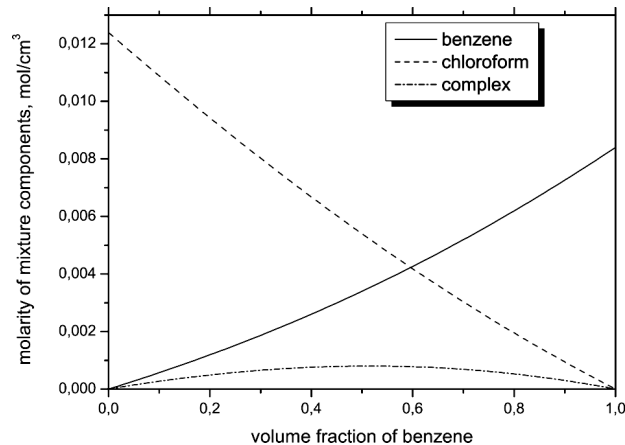
a CH bond due to the complex formation. The interpretation of the blue shift of benzene CH vibrations in the complex is not so straighforward.

4.3.2. Model-based decomposition

Our model-based analysis is based on the assumption of equimolecular complex formation, i.e. the molecular complex consists of one molecule of benzene and one molecule of chloroform. The corresponding reaction is the following [2]

$$B + C \rightleftarrows BC. \tag{13}$$

---

[2] For the sake of simplicity, we use the notation: B – benzene, C – chloroform, BC – complex.
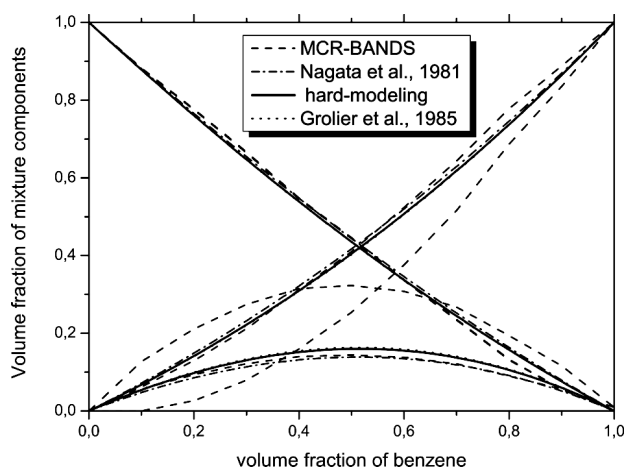
Fig. 8. Concentration profiles of benzene-chloroform mixture components obtained by different techniques

The equilibrium constant, which corresponds to this reaction, is

$$K_c = \frac{[BC]}{[B][C]}, \qquad (14)$$

where the square brackets denote the molar concentration (molarity). By solving the optimization problem (4), we found the optimal value of equilibrium constant $K_c^{\text{opt}} = 43.6$ cm^3/mol. Corresponding concentration profiles are shown in Fig. 7.

The molecular complex formation in a benzene-chloroform solution was widely studied by different techniques. In particular, NMR studies [10] gave the value of equilibrium constant $K_x = 0.36$, and the analysis of excess thermodynamic functions [16] gave the value $K_x = 0.45$. Here, K_x is the molar fraction-based equilibrium constant. All concentration profiles were rebuilt in volume fractions in order to compare the results obtained by different techniques. The resulting profiles are shown in Fig. 8. It can be seen that the hard-modeling, NMR studies, and thermodynamic analysis give similar values of the volume fraction of mixture components. At the same time, all these profiles are concentrated in the range of feasible solutions given by MCR-BANDS. It was already been indicated that the MCR-BANDS analysis is model-free. Hence, the similarity of results given by both model-free and model-based techniques confirms the adequacy of the hypothesis of equimolecular complex formation in a benzene-chloroform mixture.

5. Conclusions

The 2D correlation analysis and the analysis of residual spectra of the IR absorption spectra of liquid benzene-chloroform solutions in the range of CH stretching vibrations indicate that, apart from both free (unbonded) benzene and chloroform, there are benzene and chloroform in the bonded state. We interpret such bonded state as a molecular complex. The spectrum of the complex is highly overlapped with spectra of the pure components.

The MCR analysis supports a three-component model, i.e. we can consider the real binary solution as an effective ternary ideal solution. The decomposition of the spectral data matrix was made in two ways: model-free and model-based. The model-based decomposition was performed, by assuming that the complex consists of one molecule of benzene and one molecule of chloroform. The obtained spectral profile of the molecular complex is highly overlapped with pure component spectra, which coincides with the conclusion made by the 2D COS analysis. The concentration profiles obtained by the model-based approach and by NRM and thermodynamic studies are in a feasible range of results obtained by MCR-BANDS, which indicates the possibility of the 1:1 molecular complex formation.

1. B.E. Poling, J.M. Prausnitz, and J.P. Oonnell, *The Properties of Gases and Liquids* (McGraw-Hill, New York, 2001).
2. J. Catalan, C. Diaz, and F. Garcia-Blanco, J. Org. Chem. **65**, 3409 (2000).
3. M. Homocianu and A. Airinei, J. Mol. Liq. **209**, 549 (2015).
4. M.I. Shakhparonov, *Introduction to Modern Theory of Solutions* (Vysshaya shkola, Moscow, 1976) [in Russian].
5. L.W. Reeves and W.G. Schneider, Can. J. Chem. **35**, 251 (1957).
6. W.G. Schneider, J. Phys. Chem. **66**, 2653 (1962).
7. C.J. Creswell and A.L. Allred, J. Phys. Chem. **66**, 1469 (1962).
8. J. Homer and M.C. Cooke, J. Chem. Soc. A, **777**, 773 (1969).
9. W.T. Huntress, jr., J. Phys. Chem. **73**, 103 (1969).
10. W. Lin and S. Tsay, J. Phys. Chem. **74**, 1037 (1970).
11. W. Rothschild, Mol. Phys. **105**, 1003 (2007).
12. W.G. Rothschild, J. Mol. Liq. **150**, 68 (2009).
13. P. Boule, J. Chem. Phys. **57**, 5285 (1972).
14. M. Tamres, J. Am. Chem. Soc. **74**, 3375 (1952).
15. R.P. Rastogi, J. Nath, and R.R. Misra, J. Chem. Thermod. **3**, 307 (1971).
16. J.-P. E. Grolier, G. Roux-Desgranges, Z.S. Kooner, J.F. Smith, and L.G. Hepler, J. Sol. Chem. **16**, 745 (1987).

17. N.-Y.R. Ma and A.L. Beyerlein, J. Phys. Chem. **87**, 245 (1983).
18. H.F. Shurvel, in *Handbook of Vibrational Spectroscopy*, edited by J. Chalmers and P. Griffiths (Wiley, Chichester, 2002), p. 1783.
19. Q. Li, N. Wang, Q. Zhou, S. Sun, and Z. Yu, Appl. Spectr. **62**, 166 (2008).
20. O. Ilchehko, V. Nikonova, A. Kutsyk, and V. Obukhovsky, Ukr. J. Phys. **59**, 268 (2014).
21. I. Noda and Y. Ozaki, *Two-Dimensional Correlation Spectroscopy. Application in Vibrational and Optical Spectroscopy* (Wiley, Chichester, 2004).
22. J.-H. Jiang and Y. Ozaki, Appl. Spectr. Rev. **37**, 321 (2002).
23. N. Wang, Q. Li, and Z. Wu, Appl. Spectr. **63**, 1356 (2009).
24. N. Wang, Q.Z.F. Wu, Q. Li, and Z.Yu, J. Phys. Chem. B **114**, 8689 (2010).
25. A. de Juan and R. Tauler, Anal. Chim. Acta **500**, 195 (2003).
26. R. Tauler, A. Smilde, and B. Kowalski, J. Chemometr. **9**, 31 (1995).
27. R. Tauler, J. Chemometr. **15**, 627 (2001).
28. A. de Juan, M. Maeder, M. Martinez, and R. Tauler, Chem. Intel. Lab. Sys. **54**, 123 (2000).
29. S. Norman and M. Maeder, Crit. Rev. Anal. Chemi. **36**, 199 (2006).
30. I. Noda, Appl. Spectr. **47**, 1329 (1993).
31. I. Noda, Appl. Spectr. **54**, 994 (2000).
32. I. Noda, J. Mol. Struc. **883–884**, 216 (2008).
33. J. Jaumot, A. de Juan, and R. Tauler, Chem. Intel. Lab. Sys. **140**, 1 (2015).
34. S.A. Aivazyan, V.M. Buchstaber, I.S. Yenyukov, and L.D. Meshalkin, *Applied Statistics. Classification and Reduction of Dimensionality* (Finansy i Statistika, Moscow, 1989) (in Russian).

О.О. Ільченко, А.М. Куцик,
Ю.В. Пільгун, В.В. Обуховський, В.В. Ніконова

АНАЛІЗ КОМПЛЕКСОУТВОРЕННЯ
У РІДКИХ РОЗЧИНАХ БЕНЗОЛУ З ХЛОРОФОРМОМ
МЕТОДАМИ ІНФРАЧЕРВОНОЇ ДВОВИМІРНОЇ
КОРЕЛЯЦІЙНОЇ СПЕКТРОСКОПІЇ
ТА БАГАТОВИМІРНОГО РОЗДІЛЕННЯ КРИВИХ

Р е з ю м е

Комплексоутворення у рідкому розчині бензолу із хлороформ було досліджено методами спектроскопії інфрачервоного поглинання. Спектри виміряно в області 2950–3100 см$^{-1}$, яка відповідає області валентних CH коливань бензолу та хлороформу. Двовимірний кореляційний аналіз вказує на існування в розчині молекулярного комплексу. Аналіз спектрів залишкової інтенсивності підтверджує цей висновок. Для декомпозиції спектральних даних використано безмодельний та модельний методи. Отримано концентраційний та спектральний профіль комплексу. Аналіз показує, що комплекс складається із однієї молекули бензолу та однієї молекули хлороформу.